Characterization of Polymer Compatibility by ^{1}H Dipolar Filter Solid-State NMR under Fast Magic Angle Spinning

Xiaoliang Wang,† Qiang Gu,† Qing Sun,† Dongshan Zhou,† Pingchuan Sun,*,‡ and Gi Xue*,†

Department of Polymer Science and Engineering, The School of Chemistry and Chemical Engineering, State Key Laboratory of Coordination Chemistry, Nanjing University, Nanjing 210093, People's Republic of China, and Key Laboratory of Functional Polymer Materials, Ministry of Education, College of Chemistry, Nankai University, Tianjin 300071, People's Republic of China

Received August 13, 2007; Revised Manuscript Received October 5, 2007

ABSTRACT: Polymer compatibility was investigated by a new strategy reported in our recent communication combining preparation of an isotopically enriched polymer blend with analysis by dipolar filter ^{1}H solid-state NMR under fast magic angle spinning (MAS). Technical details concerning the optimization of the experimental conditions of this method were first discussed. The intimate segment mixing and interchain interaction in blends of deuterated polystyrene (PS-D)/hydrogenated poly(2,6-dimethyl-1,4-phenylene oxide) (PPO) were then qualitatively characterized and compared to that in PS-H/PS-D blends. It was found that the PS-D chain is in proximity to both the aromatic and the aliphatic protons of PPO chain within 0.5 nm, and it was suggested that the distance between PS-D and the aromatic ring of PPO is shorter than that between PS-D and the aliphatic side group of PPO, whereas only the proximity within 0.5 nm among aromatic rings was observed in PS-H/PS-D blends. As compared to DSC experiment, this work also demonstrates that our strategy is sensitive enough to probe the driving force of interchain compatibility between PS-D and PPO during the interfacial diffusion process of melt blending at a molecular level.

Introduction

Polymer blends are of major economic importance in the polymer industry. The physical and chemical properties of the materials depend not only on the nature of the constituent polymers but also on how intimately they are mixed.[1] Compatibility in polymer blends has received substantial attention in the past decade.[2−5] Knowledge of the spatial proximity between chains on different scales unveils information on compatibility, which has profound influence on the macroscopic properties of the final products. Various techniques including differential scanning calorimetry (DSC), transmission electron microscopy (TEM), dynamic mechanic analysis (DMA), nonradiative energy transfer (NET), and small-angle X-ray scattering (SAXS) have been extensively used to study the chain compatibility of polymer blends.[1,6−8] These techniques, however, cannot be used to directly identify the individual structures in distinct regions of a multicomponent polymer blend. Solid-state nuclear magnetic resonance (SSNMR) spectroscopy is another powerful and convenient technique to study the structure and dynamics of polymer blends.[9−13] It can be used to provide useful information about polymer microstructure due to its sensitivity to local chemical environments.[14] Furthermore, it can also be used to probe heterogeneous dynamics and to monitor morphology changes. By measuring the time scale of proton spin diffusion, the length scales in nanoscopic heterogeneities from a few nanometers up to 100 nm and the interface between different microdomains in polymer blends can be determined.[15−18] In particular, SSNMR spectroscopy based on the dipole−dipole interaction reflects molecular interactions occurring over short distances of 0.5−1.0 nm[9] and provides an ideal technique for probing chain spatial proximity or intimate mixing at a molecular level. The interchain proximity reflects important information on their compatibility in polymer blends.

A variety of SSNMR techniques have been developed to characterize polymer compatibility on the scale of 0.5−100 nm in the past decades.[9,13] Among various nuclei, ^{13}C SSNMR has been widely applied for its excellent resolution.[13,19] Intermolecular cross polarization (CP) in polymer blends containing one deuterated component was used to investigate the intimate mixing of two chains and was successfully used to characterize the compatibility of different polymers with distinguishable chemical shifts.[19,20] However, this method does not work for some polymer blends where the chemical shifts and/or the proton relaxation times of the two components are not well distinguished.[13] Furthermore, ^{13}C SSNMR requires longer experimental time and larger amount of sample as compared to ^{1}H NMR methods due to the poor sensitivity arising from the low abundance of ^{13}C. Thus, ^{1}H SSNMR is still an attractive alternative to ^{13}C due to its high sensitivity.[9,21] Traditionally, ^{1}H relaxation time measurements were a convenient method to estimate domain size and interchain compatibility in polymer blends on the scale of 20−50 nm (T_1) and 2−5 nm ($T_{1\rho}$), respectively.[12,22−24] However, the strong spin diffusion among protons limited the use of this method to determine chain compatibility on a short length scale of 0.5 nm, and it was also difficult to use in blends where the proton relaxation times of the two components were not well distinguished. Chemical-shift filter developed by Clauss et al.[15] was also used to determine chain compatibility in polymer blends where the components are all rigid and with distinguishable chemical shift. To identify chain compatibility and phase separation of polymer blends with site resolution, one can alternatively employ two-dimensional (2D) magic-angle spinning (MAS) NMR. 2D WISE[9] and recently developed novel MAD CHHC[25] experi-

* To whom correspondence should be addressed. Tel.: +86-25-83593432. Fax: +86-25-83317761. E-mail: xuegi@nju.edu.cn (G.X.); spclbh@nankai.edu.cn (P.S.).
† Nanjing University.
‡ Nankai University.

10.1021/ma071823c CCC: $37.00
Published on Web 11/15/2007

ments based on the CP between ^{1}H and ^{13}C are powerful methods to study compatibility in multicomponent polymers. However, spin diffusion among protons during CP prevents the detection of chain proximity on a short scale of 0.5 nm. Recently developed HETCOR experiments using WIM48 can suppress ^{1}H−^{1}H spin diffusion during CP and provide a novel tool to detect chain proximity at short scale of 0.5 nm, but these methods are still time-consuming and experimentally demanding.[26,27] 2D ^{1}H−^{1}H spin-exchange experiment based on CRAMPS has also attracted attention in recent years,[28] which had been used to investigate the compatibility of interpolymer complex. However, it needs distinguishable ^{1}H chemical shifts for different components. Therefore, the development of a simple and effective ^{1}H NMR experiment to determine the chain compatibility on a short length scale of 0.5 nm is still challenging, especially for polymer blends with undistinguishable chemical shifts for different components.

Among many polymer blends, the polystyrene/poly(2,6-dimethyl-1,4-phenylene oxide) (PS/PPO) has been widely studied because of the high compatibility between PS and PPO. Many different methods, such as SANS,[29,30] NMR,[17,20,25,31−34] IR,[35,36] WAXS,[37] DSC,[38,39] rheology,[40,41] etc., were used to provide structural information on different length scales. All of the evidence indicates that PS/PPO blends are compatible in all proportions and over a considerable range of molecular weights.[42,43] However, structure fluctuations were found in the blend.[17,33] Some people believed that the compatibility originated from a strong interaction between the phenyl ring of PS and phenylene ring of PPO,[33,35,36] while others believed that the driving force in the formation of the compatible blend of PS and PPO is the π-hydrogen bond between the electrodeficient methyl groups in PPO and π-orbitals in PS.[34] Note that no direct evidence has been reported on the driving force of compatibility during melt blending at a molecule level. Among all of the methods, SSNMR has shed much light on the chain compatibility of this blend. Stejskal et al.[20] used the intermolecular cross polarization in a deuterated-PS/hydrogenous-PPO blend to investigate the intimate mixing of the two components. Karasz et al.[31,32,44] used a two-dimensional ^{13}C−^{1}H correlation NMR spectrum to interpret the structure of PPO and the PS/PPO blend. To enhance the site resolution, Schmidt-Rohr et al.[25] used the two-dimensional ^{13}C−^{13}C NMR with exchange by ^{1}H spin diffusion. Liquid-state NMR measurements[34] were also conducted on PS/PPO blend; by using small molecules with structural analogy to the PS and PPO repeat units, it was suggested that the major interaction is between the PPO methyl protons and the π-orbitals of the PS rings. However, VanderHart et al. doubted this hypothesis by using proton spin diffusion experiments with multiple-pulse techniques.[17] Using ^{13}C spin relaxation measurements, Feng et al.[33] suggested that there is a strong $\pi-\pi$ electron conjugation interaction between the aromatic rings of PS and those of PPO, while the aromatic rings of PPO drive the aromatic rings of PS to move cooperatively. Therefore, detailed information about the length scale of interchain compatibility and the forces that drive compatibility needs to be further elucidated.

In a recent communication, we developed a new and general strategy to characterize the chain interpenetration in isotopic-enriched polymer glasses within a length scale of 0.5 nm,[45] which was enlightened by the pioneering work of VanderHart.[46] This method combines the preparation of the isotopically enriched polymer blends with ^{1}H dipolar filter solid-state NMR under fast magic angle spinning. The schematic diagram of the strategy is shown in Figure 1 and will be discussed in the following section. Chain interpenetration and the intimate segment mixing in polystyrene isotopic blends of hydrogenous and deuterated chains at different interpenetration degree were successfully characterized. Although one component should be deuterated in the blend, this method has the advantages of high sensitivity and simplicity of the experiment over the CP method. It is noteworthy that this method is successful even for blends like PS-D/PS-H having undistinguishable chemical shifts of the two components, which prevents traditional NMR methods from being effectively employed. Furthermore, because a high resolution ^{1}H NMR spectrum can be achieved due to the fast MAS and "deuterium-induced ^{1}H dipolar dilution" (abbreviated as DEPODIL) effect,[45,47] this method also provides a simple and alternative way to probe intermolecular interactions in polymer blends within 0.5 nm through the observation of "isolated" ^{1}H NMR signals of different groups. Motivated by this work and to further verify the universality of our NMR method, here we employ this new technique to characterize the chain compatibility and interchain interaction in deuterated polystyrene (PS-D)/hydrogenated poly(2,6-dimethyl-1,4-phenylene oxide) (PPO) blends. Technical details that significantly affect the experimental results were first discussed, and then the chain compatibility in PS-D/PPO blends with different component ratios and preparation conditions was characterized. Finally, this method was further used to investigate the interchain interaction for PS-D/PPO blends treated at different temperatures, and the NMR results were also compared to DSC measurements, which allow us to identify the interacting groups and to gain a molecular level understanding of the forces that drive compatibility during the interfacial diffusion process of melt blending.

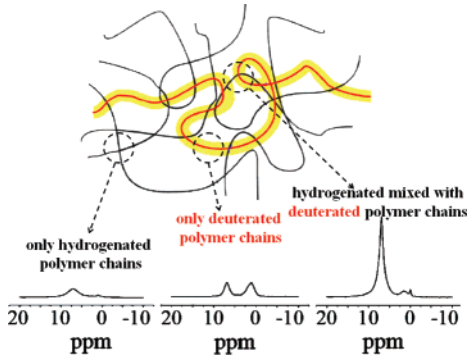

Figure 1. Schematic diagram of the NMR method for probing the chain interpenetration region in polymer glasses. The NMR spectra in this figure use PS-H/PS-D as an example.[45]

Experimental Section

The deuterated polystyrene (PS-D, Polymer Source Inc. sample no. P2404-dPS) has the number average molecule weight of 103 800, with polydispersity index of 1.38. The residual level of protonation in the PS-D is about 3.5%, as determined by liquid-state ^{1}H NMR on a Varian UNITYplus-400 NMR spectrometer at a proton frequency of 400.2 MHz. Hydrogenous poly(2,6-dimethyl-1,4-phenylene oxide) (PPO) was kindly supplied by GE Co. PS-D/PPO blends were prepared by solution blending in toluene with the polymer concentration of 5 wt %. All of the solutions were stirred overnight to ensure homogeneity.[48] The evaporation of toluene from solution proceeded slowly at 60 °C, and the weight of the sample reaches equilibrium after about 1 week. Next, the sample was dried under vacuum at 120 °C for 1 week, and a single T_g of the sample was determined by DSC measurement. The PPO and PS-D were resolved in toluene with concentration of 8 wt % separately and deposited in ethanol separately. PPO and PS-D powder were then physically mixed by mortar (abbreviation, Blend-

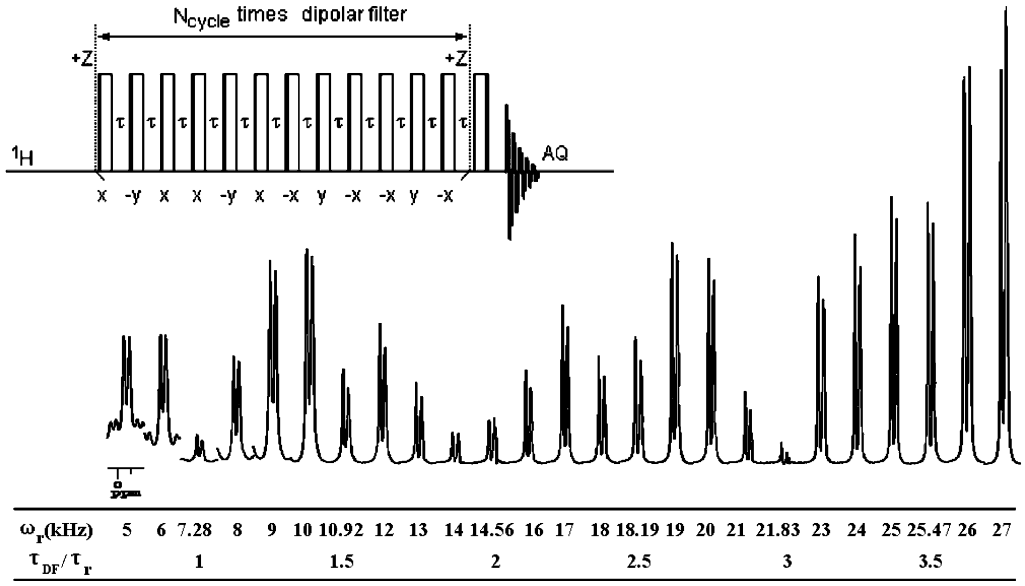

Figure 2. (top) Pulse sequence with a 12-pulse dipolar filter experiment. (bottom) The spinning-frequency dependence of the 12-pulse dipolar-filtered ^{1}H MAS spectrum on the 50/50 PS-D/PPO blend ($N_{cycle} = 8$). For each spinning frequency, the ratio of τ_{DF}/τ_r is indicated in the table, where τ_{DF} is the total cycle time of the 12-pulse dipolar filter sequence and τ_r is the rotor period.

20). Blend-20 was heated from 50 °C to the target temperature (70, 145, 250 °C) at 20 °C/min and then held at the target temperature for 10 min, finally cooling back to room temperature at 20 °C/min. The corresponding samples were abbreviated as Blend-70, Blend-145, and Blend-250, respectively. These heating processes were operated in the DSC.

Differential scanning calorimeter (DSC) measurement was carried out on a Perkin-Elmer DSC-Pyris 1 system in dry argon atmosphere. All samples were first heated from 50 to 250 °C at a rate of 20 °C/min (first heating scan) and kept at that temperature for 2 min. Subsequently, they were cooled at a rate of −20 °C/min to 50 °C and kept at 50 °C for 10 min. Next, a second scan was conducted from 50 to 250 °C with the same heating rate as the first. Temperature calibration was performed using indium as a standard. The midpoint of the slope change of the heat capacity plot was taken as the glass transition temperature (T_g).

Solid-state NMR experiments were performed on a Varian Infinityplus-400 wide-bore (89 mm) NMR spectrometer at a proton frequency of 399.7 MHz using a 2.5 mm T3 double resonance CPMAS probe, and this probe can provide stable sample spinning up to 30 kHz within ±2 Hz using a zirconia PENCIL rotor. All of the NMR data were processed with Varian Spinsight software, and all experiments were carried out at room temperature. The ^{1}H chemical shifts were referenced to external TMS. 12-Pulse dipolar filter ^{1}H experiments developed by Schmidt-Rohr et al.[49,50] as shown in the inset of Figure 2 were used to select the ^{1}H magnetization with a weak ^{1}H−^{1}H dipole−dipole interaction. The 90° pulse width was 1.45 μs, and the interpulse spacing of τ was typically 10 μs. To avoid interference between MAS and 12-pulse dipolar filter sequence, the τ value was carefully adjusted so that the dipolar filter cycle was not an integer or half integer multiple of the rotor period,[50] and a detailed discussion will be given in the following section. The spin−lattice relaxation times T_1 of protons were measured by traditional ^{13}C detected inversion recovery experiment. Recycle delays between two scans were set to five times the ^{1}H T_1 values (0.3−0.5 s). The spectra were obtained with 32 scans for each spectrum. The background signal was separately collected under the same condition without sample and then subtracted from the spectra acquired with a sample to obtain all of the spectra data used in the subsequent analysis. The sample weight in each experiment was accurately measured and was used to normalize the signal intensity. If not specified, the signal intensities were normalized by the weight of the PPO.

Results and Discussion

In our previous communication, we developed a new strategy to characterize the chain interpenetration in isotopic-enriched polymer glasses within a length scale of 0.5 nm, and a detailed description of the strategy was given.[45] For convenience of discussion in the present work, we first briefly review the three main features of this method: (1) Deuterated and hydrogenated polymers are mixed at a certain ratio. When the ^{2}H and ^{1}H nuclei are well mixed within a distance of 0.5 nm,[46] the dipole−dipole interactions among protons were significantly reduced.[47] This effect is known as "deuterium-induced ^{1}H dipolar dilution" (DEPODIL). (2) Fast MAS at 25 kHz is used to further average out the weakened ^{1}H dipole−dipole interaction in the mixing regions. (3) Dipolar filter pulse sequence is then used to suppress the signals from protons with strong dipole−dipole interactions that are out of the chain mixing regions. A unique "isolation" of ^{1}H signal can be achieved for protons that are sufficiently close to the deuterated chains on the basis of the above three steps. This isolated ^{1}H signal can be used as a sensitive probe to characterize the chain proximity in various polymer blends at a molecular level. A schematic diagram of the method is shown in Figure 1.

Optimization of the Experimental Conditions. Several factors including the interferences between MAS and 12-pulse dipolar filter sequence, the N_{cycle} value, and PS-D content significantly affect the effective application of this NMR method; we first discuss the optimization of the experimental conditions in PS-D/PPO blends and compare to previous NMR results in PS-D/PS-H blends.

(1) Interferences between MAS and the 12-Pulse Dipolar Filter Pulse Sequence. It is well known that molecular motion can destructively interfere with line-narrowing by multiple pulse techniques (such as CRAMPS) or MAS.[51−57] In principle, if the center of the correlation time distribution describing molecular motion (or proton exchange) comes close to the cycle time of the multiple pulse sequence or the integer rotor periods, the effectiveness of the multiple pulse sequences or MAS will be reduced. Although interference between multiple pulse techniques and MAS has also been reported, little work was reported on the interferences between the 12-pulse dipolar filter

pulse sequence and MAS. In our previous work, it was observed that the increase in the aromatic signal observed is not monotonic with increasing MAS frequency in isotopically enriched PS-D/PS-H blends.[45] Because the ability to average out the dipolar interactions via MAS is a monotonic function of the MAS frequency, the above NMR result implies that interferences between MAS and 12-pulse sequences should exist. Figure 2 shows the dipolar-filtered ^{1}H NMR spectra of 50/50 PS-D/PPO blend at spinning frequencies ranging from 5 to 27 kHz in step of 1 kHz and at N_{cycle} of 8. It was observed that the intensity of the dipolar-filtered ^{1}H signal strongly depends on the spinning frequency. Both the aromatic and the aliphatic groups show similar behavior, which is different from those observed in PS-D/PS-H blends, and this difference will be discussed in the following section. For each spinning speed, the ratio τ_{DF}/τ_r (where τ_{DF} is the total cycle time of the 12-pulse dipolar filter sequence, i.e., $12*(1.45 + 10) = 137.4$ μs, and τ_r the rotor period) is indicated in the table. As illustrated in Figure 2, we can see that the increase in dipolar-filtered signal is not monotonic with increasing MAS frequency. At rotor spinning frequencies of 7.28, 14.56, and 21.83 kHz, we observe obvious decreases of the ^{1}H signal intensity. These three spinning frequencies correspond to an integer ratio τ_{DF}/τ_r of 1, 2, and 3, respectively. These special ratios between the cycle time and rotor period are likely to correspond to strong ^{1}H−^{1}H dipolar interaction and chemical-shift anisotropy recoupling conditions, as already observed by Filip and Hafner for the windowless WHH-4 sequency,[53] or by Lesage et al. for continuous phase modulation multiple-pulse DUMBO-1 sequence.[58] In addition, it is also noted that an obvious decrease of the signal intensity is also observed at half integer (1.5, 2.5) of τ_{DF}/τ_r. These recoupling windows can be easily avoided by adjusting the interpulse spacing (τ) in the dipolar filter sequence, so that the dipolar filter cycle was not an integer or half integer multiple of the rotor period. It is noteworthy that the dipolar-filtered signal is not sensitive to the spinning frequency higher than 23 kHz. Therefore, the automatic control of the MAS frequency at high spinning rate of 25 kHz and fine adjustment of the interpulse spacing of τ in 12-pulse dipolar filter sequence are crucial to guarantee the accurate measurement of the dipolar-filtered ^{1}H signal.

(2) The Influence of N_{cycle} Value and PS-D Content on the 12-Pulse Dipolar Filtered ^{1}H MAS Spectrum. The fraction of the detected protons after the dipolar filter depends strongly on the strength of the dipolar filter (selection of N_{cycle}) employed. To obtain a better understanding of the influence of N_{cycle} values on the spectrum, we have investigated the N_{cycle} value dependence of the signal intensities and line shape in different samples. The spectra of pure PPO, 50/50 PS-D/PPO blend, and pure PS-D at N_{cycle} values from 0 to 10 were shown in Figure 3. We can see that the intensities from the pure PPO decreased dramatically with increasing N_{cycle} values, and the signals are almost completely suppressed at N_{cycle} larger than 8. This implies that the ^{1}H−^{1}H dipole−dipole interactions among protons should be very strong in hydrogenous PPO even at the fast spin frequency of 25 kHz. On the other hand, the signal intensity of the pure PS-D is only slightly decreased with increasing N_{cycle} as shown in Figure 3b (the corresponding integration versus N_{cycle} was shown in Figure 4). Because the residual level of protonation in the PS-D is about 3.5%, this means that ^{1}H−^{1}H dipole−dipole interaction among residual proton is very weak and could be averaged out under fast MAS condition. In the case of 50/50 wt % PS-D/PPO blend as shown in Figure 3c, the signal intensity from 50/50 PS-D/PPO decreases slower with

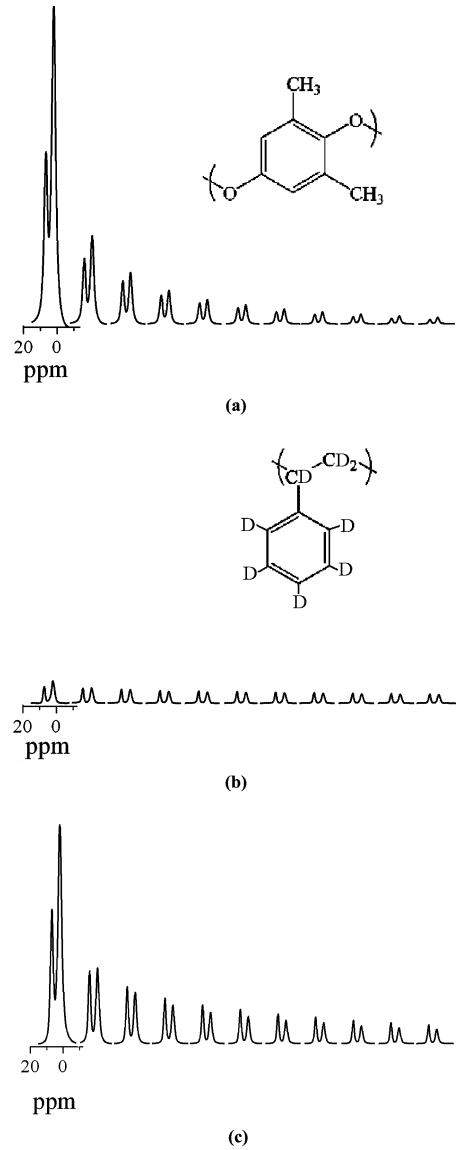

Figure 3. The ^{1}H dipolar-filtered MAS NMR spectrum of (a) PPO (inset is the molecular formula of PPO), (b) PS-D with residual protons (inset is the molecular formula of PS-D), and (c) the blend of 50/50 wt % PS-D/PPO with 12-pulse dipolar filter at N_{cycle} values from 0 to 10 (from left to right) at room temperature and spinning frequency of 25 kHz. The spectra were normalized by PPO sample weight, and the corresponding spectra of PS-D in these figures were normalized by PS-D sample weight and used to show the effect of residual protons.

increasing N_{cycle} when compared to pure PPO (Figure 3a), which implies that some of the signal due to the DEPODIL effect in this isotopically enriched blend could be partly isolated. To confirm this conclusion, we further compare the spectra of PPO, PS-D, 50/50 PS-D/PPO physical mixture, and 50/50 PS-D/PPO cast blends ($N_{cycle} = 8$) in Figure 4. We can see that the signal from the PS-D/PPO physical mixture shows nothing special but the simple linear sum of the PPO and PS-D signals. For the 50/50 PS-D/PPO cast blend, however, both signals from aromatic protons and aliphatic protons increase significantly. Furthermore, we can also notice that the increment of the signal from aromatic protons is larger than that from aliphatic protons.

The intensity of the observed isolated signals of the hydrogenous chains after dipolar filter depends strongly on the number of deuterated chains that closely surrounded it. To obtain the most effective content of the deuterated chains in dipolar-filtered ^{1}H MAS experiments, we prepared three PS-D/PPO blends with weight ratios of 25/75, 50/50, and 75/25, respectively. Figure 5

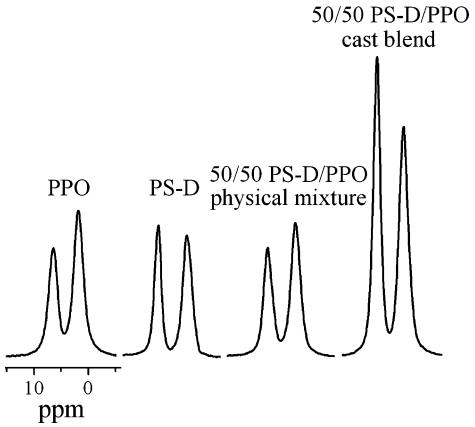

Figure 4. The dipolar-filtered ^{1}H MAS NMR spectra of PPO, PS-D, 50/50 PS-D/PPO physical mixture, and 50/50 PS-D/PPO cast blend. It was recorded at room temperature with 12-pulse dipolar filter at N_{cycle} = 8 and 25 kHz spinning frequency. The intensities were normalized by the total sample weight in the rotor.

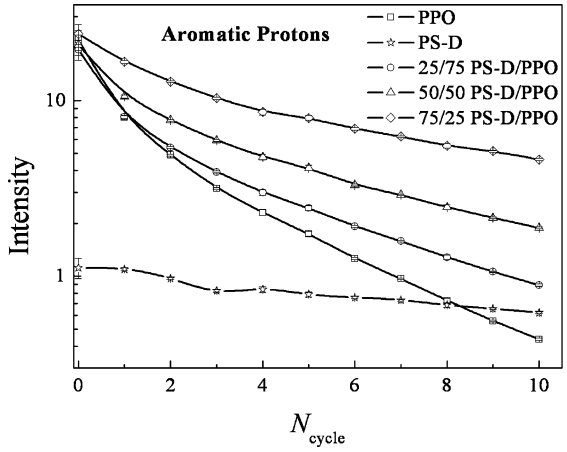

(a)

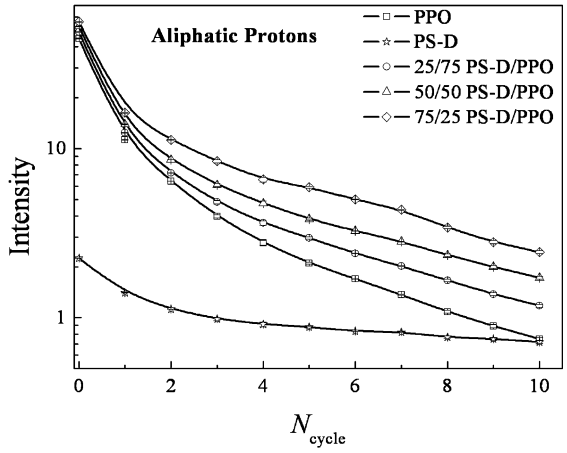

(b)

Figure 5. The integration of the proton signal from aromatic ring (a) and the aliphatic side group (b) of PPO versus the N_{cycle} of different samples. To compare the isolated signal, the integration was normalized by the weight of PPO after the contribution of the residual proton in PS-D was subtracted in the corresponding blend.

shows the integral intensities of the proton signal from aromatic ring and the aliphatic side group of PPO versus the N_{cycle} of different samples. To compare the isolated signal, the integration was normalized by the weight of PPO after the contribution of the part from the residual proton in PS-D was subtracted in the corresponding blends. So the difference in the signal intensities between the blends and pure PPO at the same N_{cycle} value reflects the relative amount of isolated proton signal. We can see that the integration values of different blends and pure PPO are nearly equal at $N_{cycle} = 0$. This indicates that no obvious difference appears if all proton signals of the samples were detected without using dipolar filter. With the increasing N_{cycle} value, the signals with strong ^{1}H−^{1}H dipole−dipole interactions were suppressed, while the signals from the protons proximate to the PS-D chains were isolated due to the DEPODIL effect. We can see that the relative intensities of the isolated aromatic and aliphatic signals increase with increasing PS-D content at the same N_{cycle} value. This is the direct NMR evidence that the PS-D chains are intimately mixed with both aromatic and aliphatic protons of PPO within a distance of 0.5 nm.

In Figure 5a, we can see that the signal from pure PPO remains considerably large for $N_{cycle} < 8$, so the fractions of signal in the blends coming from PPO protons that do not belong to the chain interpenetration regions cannot be neglected. These proton signals mask the effective NMR signal, reflecting the degree of chain interpenetration between different blends. It is noteworthy that when $N_{cycle} > 8$, the signal of pure hydrogenous PPO is almost completely suppressed. Meanwhile, the isolated proton signal of hydrogenous PPO chains, in which protons are sufficiently close to the ^{2}H nuclei of deuterated PS chains in the PS-D/PPO blends, becomes weaker. It should be also noted that, when $N_{cycle} > 8$, the fraction of the observed protons is not strong enough to give reasonable signal intensity, and the contribution from the residual aromatic protons in PS-D is considerably large. As the result, eight is the optimized N_{cycle} value to be selected in our experiments. In addition, we mentioned in our previous work that the presence of a small amount of residual protons does not interfere with the experimental results.[45] Figure 6 shows the corresponding spectra of Figure 5 at $N_{cycle} = 4$ and 8, respectively. It is clear that the spectral contrast of $N_{cycle} = 8$ is better than that of $N_{cycle} = 4$, in agreement with the above discussion. From Figures 4 and 5, we can see that the isolated proton signal of the 75/25 PS-D/PPO was the strongest within the three blends, which indicates that 75% is the most effective PS-D content in PS-D/PPO blends. In our previous work on PS-D/PS-H blends, we found that the effective PS-D content is 50%, which is smaller than that in PS-D/PPO blends. The different optimal deuterated sample content between different blends originates from the interchain interaction, which will be discussed in the following section. This indicates that the effective PS-D content in different blends should be carefully adjusted. On the basis of the above discussions, the optimized experimental conditions can be determined and used in the following work. In addition, it should be also noted that the selection actually done by the dipolar filter should be carefully checked in samples with weak dynamic contrast as suggested in a recent report by Spiess et al.[59]

Interchain Interaction in PS-D/PPO Blends. Figure 6 shows the dipolar-filtered ^{1}H MAS NMR spectra of PPO, PS-D, 25/75, 50/50, 75/25 PS-D/PPO blends, and 50/50 PS-D/PPO physical mixture recorded at N_{cycle} equals (a) 4 and (b) 8, respectively. From Figure 6, it is clearly demonstrated that high-resolution ^{1}H NMR spectrum can be achieved due to the fast MAS and DEPODIL effect,[45] which provides us with a simple and alternative way to probe intermolecular interactions in polymer blends within 0.5 nm through the observation of isolated ^{1}H NMR signals of different groups.

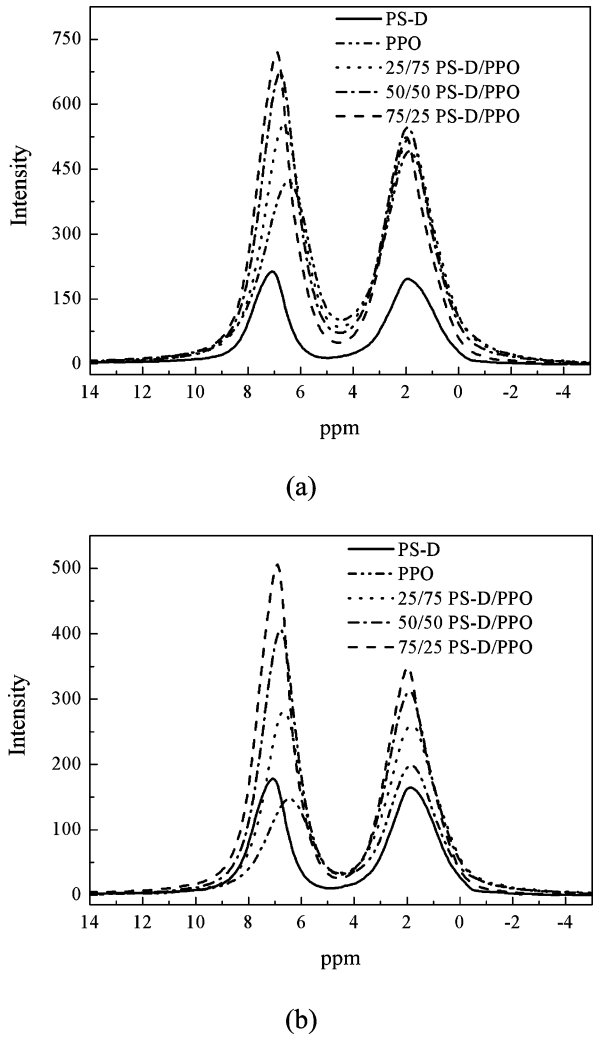

Figure 6. The dipolar-filtered ^{1}H MAS NMR spectra of PPO, PS-D, 25/75, 50/50, 75/25 PS-D/PPO blends, and 50/50 PS-D/PPO physical mixture recorded at N_{cycle} equals (a) 4 and (b) 8, respectively. The spectra were normalized by PPO sample weight, and the corresponding spectra of PS-D in these figures were normalized by PS-D sample weight and used to show the effect of residual protons.

First, the interchain interaction can be determined by comparison of the peak intensity of the aliphatic and aromatic groups. From the spectrum of pure PPO in Figure 6, it is shown that the signal from aliphatic protons is stronger than the signal from aromatic protons because the amount of aliphatic protons is larger than the amount of aromatic protons from their chemical structure. In the case of PS-D, the signal from residual aliphatic protons is nearly equal to the signal from residual aromatic protons. However, for PS-D/PPO blend, the signal from aromatic protons becomes stronger than that from the aliphatic protons. This indicates that the DEPODIL effect was stronger for the aromatic protons than for the aliphatic protons of PPO. Because the DEPODIL effect depends strongly on the distance between the neighbor of the deuterated and protonated chain, we can conclude that the distance between PS-D and the aromatic ring of PPO is shorter than that between PS-D and the aliphatic side group.

Second, the interchain interaction can also be determined by comparison of the chemical shifts of the aliphatic and aromatic groups. In Figure 6b at $N_{cycle} = 8$, we can see that the signal increased dramatically with increasing PS-D ratio when PS-D and PPO are cast from toluene solution and are guaranteed to form compatible blends.[33,39] With the increase of PS-D ratio, the chemical shift of the aromatic peak moves from 6.4 to 7.0 ppm, which are assigned to the signal from aromatic protons of pure PPO and pure PS, respectively. This result also clearly indicates the presence of the strong interaction between aromatic rings of PPO and PS-D and is in good agreement with the results from the above discussion.

Third, the interchain interaction can also be determined by comparison of the slopes of the curves shown in Figure 5. In this figure, the slopes of the curves reflect the decay speed of the signal under ^{1}H dipolar filter: the flatter the slope is, the slower the decay speed is, which means more signal is isolated in the blends, and vice versa. It is noteworthy that the slopes of the curves for aromatic signals in PS-D/PPO blends (Figure 5a) are flatter than those of the corresponding aliphatic signals (Figure 5b). This indicates that the DEPODIL effect in aromatic protons signals is stronger than that in aliphatic proton signals. Because the DEPODIL effect depends strongly on the distance between ^{2}H and ^{1}H, this suggests that the distance between the aromatic ring of PPO and PS-D is closer than that between the aliphatic protons of PPO and deuterium of PS-D.

It was reported that the major interaction was between the PPO methyl protons and the π-orbitals of the PS rings as suggested by some liquid-state NMR measurements[34] using small molecules with structural analogy to the PS and PPO repeat units. However, VanderHart casts doubts on this hypothesis.[17] Using ^{13}C spin relaxation measurements, Feng et al.[33] suggested that there was a strong $\pi-\pi$ electron conjugation interaction between the aromatic rings of PS and those of PPO, while the aromatic rings of PPO drive the aromatic rings of PS to move cooperatively. Our results suggest that the interaction between the PPO methyl protons and the π-orbitals of the PS rings may exist but would not be predominant.

It is interesting to note that both signals from the aromatic ring and aliphatic protons are isolated in PS-D/PPO blends; this behavior is quite different from that observed in our previous work on PS-H/PS-D blends,[45] where only the signal from aromatic proton could be isolated. On the basis of the above discussion on PS-D/PPO blends, we ascribed this difference between the PS-H/PS-D and PS-D/PPO blends to their different interchain interactions. It was reported that a correlation length of 0.5−0.6 nm was favored for PS-d5/PS-d3 blends simulated based on the Gaussian correlation model through the experimental spin diffusion data.[31] In our previous work of PS-H/PS-D, it was observed that the signal from the aromatic ring was isolated by the deuterated PS while the aliphatic proton was not, and this was ascribed to the spatial obstruction[46,60] of the aromatic groups to the protons of the main chain: the PS-D no longer has the chance to be near the aliphatic protons within the effective distance to induce "^{1}H dipolar dilution" in PS-H/PS-D blends. On the other hand, for PS-D/PPO blend, the phenylene rings of PPO are approximately perpendicular,[44] the PS-D has the chance to near both the aromatic protons and the aliphatic protons,[37] and both the aromatic protons and the aliphatic protons could be isolated by the PS-D. Furthermore, it was reported that the shortest distance between the protons of PPO and PS segments in adjacent lattice sites of PS/PPO segment is 0.33 nm,[32] and there is a correlation length of 0.4 nm for the PPO/PS-d3 blends.[31] Therefore, the correlation length of PPO/PS is shorter than that of PS-d3/PS-d5 (0.5−0.6 nm). Shorter correlation length implies that the deuterated PS chains are more proximate to the PPO than to the PS-H chains, and this should be the main reason of the different behavior of the DEPODIL effect observed in these two isotopically enriched polymer blends.

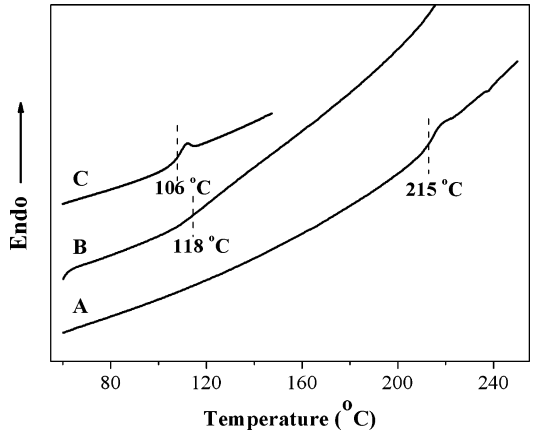

Figure 7. The DSC traces (second heating scan) of (A) PPO, (B) physical mixture of PS-D and PPO, and (C) PS-D. After a heating history from 50 to 250 °C with 20 °C/min and holding at 250 °C for 10 min, the physical mixture of PS-D and PPO with equal weights shows a single T_g of 118 °C.

Chain Compatibility during Melt Blending. Compatible polymer blends are usually diagnosed as such by their single T_g's and transparency. These criteria, even though practical, only imply a homogeneity on a scale of tens of nanometers or larger.[1] As shown in Figure 7, DSC was used to characterize the intimate mixing of the two different chains in physical mixture of PS-D and PPO with equal weights, after heating from 50 to 250 °C at 20 °C/min and then holding at 250 °C for 10 min as a simple process of melt blending (Blend-250). The Blend-250 had a broad and not well-distinguished mutual glass transition temperature of 118 °C. The T_g of the solution cast PS-D/PPO 50/50 blend is 146 °C (not show here), which well agreed with others'.[38,39] The difference between the T_g of the two samples should originate from the level of compatibility. The segmental mixing occurs only in the interfacial regions between the PS-D and PPO powder in Blend-250, while the segmental mixing occurs homogenously at a molecular level in solution cast blend. The single glass transition temperature suggests good compatibility in these blends, even in Blend-250. However, the driving force of interchain compatibility between PS-D and PPO during the melt blending process of such compatible blends is less understood. To investigate the interacting groups and to gain a molecular level understanding of the forces that drive compatibility during the process of melt blending, we further employed the ^{1}H dipolar filter NMR method on the sample with different heating history: heating from 50 °C to target temperature (70, 145, 250 °C) at 20 °C/min and then holding at the target temperature for 10 min, finally cooling back to room temperature at 20 °C/min (Blend-70, Blend-145, and Blend 250). The results are shown in Figure 8. It is interesting to note that there is no special change in the spectra of Blend-20, Blend-70, and Blend-145, in which the aging temperature is below the glass transition temperature of the pure PPO. In the spectrum of Blend-250, both signals from the aromatic and aliphatic protons increased significantly. This indicates that the significant compatible process occurred at interface only when the two polymer chains obtain enough segmental scale mobility upon heating. This means that blending below the T_g of one component should not result in a mixing better than physical blending at room temperature. The interdiffusion of polymer chains between the powder interface occurs above the T_g of the involved polymers.[61−63] As compared to the relative integral intensity of the corresponding signal from the Blend-20, the signal intensity increased 75% for aromatic protons, while 43% for aliphatic protons. This result semiquantitatively indicates that the interaction between the aromatic protons of PPO and PS-D is stronger than that between aliphatic protons and PS-D during the aging process. On the other hand, it also means that the strong interaction between the phenyl ring of PS and phenylene ring of PPO is the key factor driving compatibility during interface diffusion. This conclusion is in good agreement with our foregoing conclusion for PS-D/PPO samples cast from toluene solution. From the solution cast blend PS-D/PPO 50/50 in Figure 4, the signal intensity increased 125% for aromatic protons, while 65% for the aliphatic protons, when compared to the corresponding physical mixture. The increment of the signal intensity of solution cast blend was considerable larger than that of Blend-250. This NMR result directly explained why the Blend-250 has a broader T_g than that of the cast film. As compared to DSC experiment, this NMR method is sensitive enough to reveal the interchain interaction and intimate mixing process of polymer blends by means of interface diffusion at a molecular level.

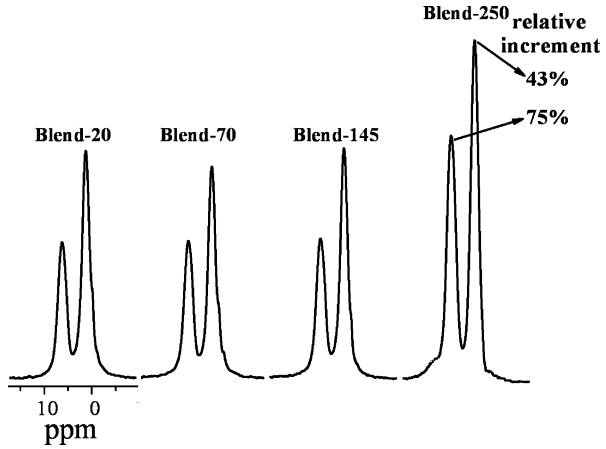

Figure 8. The spectra of Blend-20, Blend-70, Blend-145, and Blend-250 were recorded at room temperature with 12-pulse dipolar filter at $N_{cycle} = 8$ and 25 kHz spinning frequency.

Conclusions

In this work, a new strategy reported in our recent communication was further used to investigate the chain compatibility in PS-D/PPO polymer blends. Factors including the interferences between MAS and 12-pulse dipolar filter sequence, the N_{cycle} value, and PS-D content that significantly affect the effective application of this NMR method were first systematically discussed. The intimate segment mixing and interchain interaction in blends were then qualitatively characterized. It was found that the deuterated PS-D chain is in the proximity to both the aromatic and the aliphatic protons of PPO chain within 0.5 nm. Furthermore, the distance between PS-D and the aromatic ring of PPO is shorter than that between PS-D and the aliphatic side group of PPO. We confirmed that the strong interaction between the phenyl ring of PS and phenylene ring of PPO is the key factor driving compatibility during interface diffusion. By using this strategy, it is possible to identify the interacting groups and to gain a molecular level understanding of the forces that drive compatibility during the process of melt blending. These NMR studies demonstrate that the present NMR method is robust for characterizing the chain interpenetration in homopolymer glasses and chain compatibility in polymer blends even though their chemical shifts are completely undistinguishable for the two components, which is extremely challenging for traditional NMR techniques. In particular, the achievement of the high-resolution ^{1}H NMR spectrum enables us to elucidate the intermolecular interaction in polymers and other organic solids at short length scale of 0.5 nm.

Acknowledgment. We are grateful to Dr. Qiang Wang for his revision of this manuscript. This work was supported by the National Science Foundation of China (Grants 50533020, 90403013, 20374027, 20504014, 20374031), National Basic Research Program of China (Grant 2007CB925101), and the Foundation for the Author of National Excellent Doctoral Dissertation of P. R. China (Grant 200528).

References and Notes

(1) Paul, D. R.; Bucknall, C. B. *Polymer Blends: Formulation & Performance*; John Wiley & Sons, Inc.: New York, 2000.
(2) Hussein, I. A. *Macromolecules* **2003**, *36*, 4667.
(3) Yi, J. Z.; Goh, S. H.; Wee, A. T. S. *Macromolecules* **2001**, *34*, 4662.
(4) Kuo, S. W.; Chang, F. C. *Macromolecules* **2001**, *34*, 5224.
(5) Eisenbach, C. D.; Hofmann, J.; Godel, A.; Noolandi, J.; Shi, A. C. *Macromolecules* **1999**, *32*, 1463.
(6) Ferry, J. D. *Viscoelastic Properties of Polymers*, 3rd ed.; John Wiley & Sons, Inc.: New York, 1980.
(7) Morawetz, H. *Science* **1988**, *240*, 172.
(8) Chu, B.; Hsiao, B. S. *Chem. Rev.* **2001**, *101*, 1727.
(9) Schmidt-Rohr, K.; Spiess, H. W. *Multidimensional Solid-State NMR and Polymers*; Academic Press Inc.: San Diego, CA, 1994.
(10) VanderHart, D. L.; Manley, R. S. J.; Barnes, J. D. *Macromolecules* **1994**, *27*, 2826.
(11) Mulder, F. M.; Jansen, B. J. P.; Lemstra, P. J.; Meijer, H. E. H.; de Groot, H. J. M. *Macromolecules* **2000**, *33*, 457.
(12) Wagler, T.; Rinaldi, P. L.; Han, C. D.; Chun, H. *Macromolecules* **2000**, *33*, 1778.
(13) Guo, M. M. *Trends Polym. Sci.* **1996**, *4*, 238.
(14) Tonelli, A. E. *NMR Spectroscopy and Polymer Microstructure*; VCH: New York, 1989.
(15) Clauss, J.; Schmidt-Rohr, K.; Spiess, H. W. *Acta Polym.* **1993**, *44*, 1.
(16) Landfester, K.; Spiess, H. W. *Acta Polym.* **1998**, *49*, 451.
(17) VanderHart, D. L. *Macromolecules* **1994**, *27*, 2837.
(18) Cherry, B. R.; Fujimoto, C. H.; Cornelius, C. J.; Alam, T. M. *Macromolecules* **2005**, *38*, 1201.
(19) Guo, M.; Zachmann, H. G. *Polymer* **1993**, *34*, 2503.
(20) Stejskal, E. O.; Schaefer, J.; Sefcik, M. D.; McKay, R. A. *Macromolecules* **1981**, *14*, 275.
(21) Schnell, I.; Spiess, H. W. *J. Magn. Reson.* **2001**, *151*, 153.
(22) Ibbett, R. N. *NMR Spectroscopy of Polymers*; Blackie Academic & Professional: 1993.
(23) Henrichs, P. M.; Tribone, J.; Massa, D. J.; Hewitt, J. M. *Macromolecules* **1988**, *21*, 1282.
(24) Adriaensens, P.; Storme, L.; Carleer, R.; Gelan, J.; Du, Prez, F. E. *Macromolecules* **2002**, *35*, 3965.
(25) Hou, S. S.; Chen, Q.; Schmidt-Rohr, K. *Macromolecules* **2004**, *37*, 1999.
(26) Rusa, C. C.; Tonelli, A. E. *Macromolecules* **2000**, *33*, 5321.
(27) Jia, X.; Wolak, J.; Wang, X. W.; White, J. L. *Macromolecules* **2003**, *36*, 712.
(28) Brus, J.; Petrickova, H.; Dybal, J. *Solid State Nucl. Magn. Reson.* **2003**, *23*, 183.
(29) Maconnachie, A.; Kambour, R. P.; White, D. M.; Rostami, S.; Walsh, D. J. *Macromolecules* **1984**, *17*, 2645.
(30) Wignall, G. D.; Child, H. R.; Liaravena, F. *Polymer* **1980**, *21*, 131.
(31) Li, S.; Rice, D. M.; Karasz, F. E. *Macromolecules* **1994**, *27*, 6527.
(32) Li, S.; Rice, D. M.; Karasz, F. E. *Macromolecules* **1994**, *27*, 2211.
(33) Feng, H. Q.; Feng, Z. L.; Ruan, H. Z.; Shen, L. F. *Macromolecules* **1992**, *25*, 5981.
(34) Djordjevic, M. B.; Porter, R. S. *Polym. Eng. Sci.* **1983**, *23*, 650.
(35) Wellinghoff, S. T.; Koenig, J. L.; Baer, E. *J. Polym. Sci., Part B: Polym. Phys.* **1977**, *15*, 1913.
(36) Lefebvre, D.; Jasse, B.; Monnerie, L. *Polymer* **1981**, *22*, 1616.
(37) Mitchell, G. R.; Windle, A. H. *J. Polym. Sci., Part B: Polym. Phys.* **1985**, *23*, 1967.
(38) Shultz, A. R.; Gendron, B. M. *J. Appl. Polym. Sci.* **1972**, *16*, 461.
(39) Shultz, A. R.; McCullou, Cr. *J. Polym. Sci., Part B: Polym. Phys.* **1972**, *10*, 307.
(40) Prest, W. M.; Porter, R. S. *J. Polym. Sci., Part B: Polym. Phys.* **1972**, *10*, 1639.
(41) Messe, L.; Prud'homme, R. E. *J. Polym. Sci., Part B: Polym. Phys.* **2000**, *38*, 1405.
(42) Stoeltin, J.; Karasz, F. E.; Macknigh, W. *Polym. Eng. Sci.* **1970**, *10*, 133.
(43) Shultz, A. R.; Beach, B. M. *Macromolecules* **1974**, *7*, 902.
(44) Bielecki, A.; Burum, D. P.; Rice, D. M.; Karasz, F. E. *Macromolecules* **1991**, *24*, 4820.
(45) Wang, X. L.; Tao, F. F.; Sun, P. C.; Zhou, D. S.; Wang, Z. Q.; Gu, Q.; Hu, J. L.; Xue, G. *Macromolecules* **2007**, *40*, 4736.
(46) VanderHart, D. L.; Manders, W. F.; Stein, R. S.; Herman, W. *Macromolecules* **1987**, *20*, 1724.
(47) Mehring, M. *Principles of High Resolution NMR in Solid*, 2nd ed.; Springer-Verlag, Inc.: Berlin Heidelberg, New York, 1983.
(48) Devotta, I.; Badiger, M. V.; Rajamohanan, P. R.; Ganapathy, S.; Mashelkar, R. A. *Chem. Eng. Sci.* **1995**, *50*, 2557.
(49) Egger, N.; Schmidt-Rohr, K.; Blumich, B.; Domke, W. D.; Stapp, B. *J. Appl. Polym. Sci.* **1992**, *44*, 289.
(50) Sun, P. C.; Dang, Q. Q.; Li, B. H.; Chen, T. H.; Wang, Y. N.; Lin, H.; Jin, Q. H.; Ding, D. T.; Shi, A. C. *Macromolecules* **2005**, *38*, 5654.
(51) Demco, D. E.; Hafner, S.; Spiess, H. W. *J. Magn. Reson., Ser. A* **1995**, *116*, 36.
(52) Hafner, S.; Demco, D. E. *Solid State Nucl. Magn. Reson.* **2002**, *22*, 247.
(53) Filip, C.; Hafner, S. *J. Magn. Reson.* **2000**, *147*, 250.
(54) Hafner, S.; Spiess, H. W. *Concepts Magn. Reson.* **1998**, *10*, 99.
(55) McDermott, A.; Ridenour, C. F. *The Encyclopedia of NMR*; Wiley: London, 1997.
(56) Liu, C. H. C.; Maciel, G. E. *Anal. Chem.* **1996**, *68*, 1401.
(57) Mirau, P. A.; Yang, S. *Chem. Mater.* **2002**, *14*, 249.
(58) Lesage, A.; Sakellariou, D.; Hediger, S.; Elena, B.; Charmont, P.; Steuernagel, S.; Emsley, L. *J. Magn. Reson.* **2003**, *163*, 105.
(59) Gaborieau, M.; Graf, R.; Spiess, H. W. *Solid State Nucl. Magn. Reson.* **2005**, *28*, 160.
(60) Mitchell, G. R.; Windle, A. H. *Polymer* **1984**, *25*, 906.
(61) Wang, Y. C.; Winnik, M. A. *J. Phys. Chem.* **1993**, *97*, 2507.
(62) Oh, J. K.; Tomba, P.; Ye, X. D.; Eley, R.; Rademacher, J.; Farwaha, R.; Winnik, M. A. *Macromolecules* **2003**, *36*, 5804.
(63) Wool, R. P. *Polymer Interface*; Hanser Publishers: Munich, 1995.

MA071823C